European Journal of Nuclear Medicine and Molecular Imaging (2020) 47:1083–1093
https://doi.org/10.1007/s00259-019-04632-w

ORIGINAL ARTICLE

^{18}F-FDG PET/CT in diagnostic and prognostic evaluation of patients with cardiac masses: a retrospective study

Chunxia Qin[1,2] · Fuqiang Shao[1,2] · Fan Hu[1,2] · Wenyu Song[1,2] · Yangmeihui Song[1,2] · Jinxia Guo[3] · Xiaoli Lan[1,2]

Received: 28 September 2019 / Accepted: 18 November 2019 / Published online: 5 December 2019

Abstract

Purpose Correct diagnosis and prognostic assessment of cardiac masses are crucial before therapy. We evaluated the diagnostic and prognostic value of ^{18}F-FDG PET/CT in patients with cardiac masses.

Methods ^{18}F-FDG PET/CT images of 64 patients with 65 cardiac masses were retrospectively analysed (34 men, 30 women; average age, 51.2 ± 17.5 years). Comparisons of CT features and ^{18}F-FDG metabolic indices between benign and malignant entities, as well as among primary and secondary malignancies and lymphoma, were performed. The diagnostic values of PET/CT for distinguishing benign versus malignant masses were calculated. PET/CT data were further assessed for the predictive value for overall survival (OS) using the Cox proportional hazards model to assess potential independent predictors. Kaplan-Meier curves were generated to assess the value of PET/CT for prognostication.

Results Statistically significant differences in various morphological features and metabolic indices between benign and malignant masses were found. An SUV_{max} of 6.75 was the optimal cutoff value to differentiate between benign and malignant masses, and the diagnostic sensitivity, specificity, accuracy, positive predictive value, and negative predictive value were 92.11%, 88.89%, 90.77%, 92.11%, and 88.89%, respectively. Taking CT features and $SUV_{max} \geq 6.75$ as a criterion, the values were 76.32%, 100.00%, 86.15%, 100.00%, and 75.00%, respectively; taking ≥ 3 CT features or $SUV_{max} \geq 6.75$ as a criterion, the values were 94.74%, 88.89%, 92.31%, 92.31%, and 92.31%, respectively, indicating optimal diagnostic performance when paired with the anatomic information provided by the CT component. A univariate analysis of OS determined that surrounding tissue infiltration, epicardial infiltration, necrosis, multiple chambers or vessel involvement, distant metastasis, SUV_{max}, SUV_{mean}, metabolic tumour volume (MTV), and total lesion glycolysis (TLG) were significant predictors of survival. In the multivariate analysis, only $SUV_{max} \geq 6.715$ was significant ($P < 0.01$). Median OS was 1460 days for $SUV_{max} < 6.715$ and 342 days for $SUV_{max} \geq 6.715$ ($P < 0.01$).

Conclusion ^{18}F-FDG PET/CT is helpful in the diagnosis of cardiac masses before treatment and has value in detecting extracardiac primary or secondary tumours. ^{18}F-FDG PET/CT could also be a promising tool to provide prognostic information for these patients, especially SUV_{max} displaying independent prognostic value.

Keywords ^{18}F-FDG · PET/CT · Cardiac masses · Diagnosis · Prognosis

Chunxia Qin and Fuqiang Shao contributed equally to this work.

This article is part of the Topical Collection on Miscellanea

✉ Xiaoli Lan
LXL730724@hotmail.com

[1] Department of Nuclear Medicine, Union Hospital, Tongji Medical College, Huazhong University of Science and Technology, No. 1277 Jiefang Ave, Wuhan 430022, China

[2] Hubei Province Key Laboratory of Molecular Imaging, Wuhan 430022, China

[3] GE Healthcare, Shanghai, China

Introduction

Cardiac masses are rare entities with high rates of morbidity and mortality. There are three basic types: tumour, thrombus, and vegetation. Primary tumours account for an extremely small proportion, with an autopsy frequency between 0.001 and 0.3% [1]. More than three-quarters of primary neoplasms are benign and almost half of the benign neoplasms are myxomas. About 20% of primary cardiac tumours are malignant, and 95% of these are sarcomas [2]. Metastatic disease, which typically originates from a primary pulmonary tumour [3], is much more common than primary cardiac tumours.

The therapeutic strategies and prognosis of cardiac masses not only depend on the nature of the mass (neoplastic or non-neoplastic), but, in the case of neoplasm, also on the tumour characteristics (benign or malignant, primary or secondary) [4]. Because of the location, even benign cardiac masses could lead to serious consequences, such as heart failure caused by heart cavity obstruction, pulmonary/systemic embolism, and even sudden death [4, 5]. With the development of modern medical technology, the resection rate of cardiac masses has been constantly improving [4]. Adjunctive therapy can significantly reduce any impairment of cardiac function [6]. In malignancies, postoperative radiotherapy and chemotherapy can significantly improve the short-term prognosis, but the long-term prognosis remains poor [6, 7]. Correct identification of the nature of a cardiac mass by non-invasive imaging is critical for diagnosis, management strategy, and prognosis.

Anatomical imaging modalities, including transthoracic and transoesophageal echocardiography, computed tomography (CT), and magnetic resonance (MR), are valuable to provide location and structural information. However, their ability to provide metabolic information is limited [8–10]. ^{18}F-Fluorodeoxyglucose positron emission tomography/computed tomography (^{18}F-FDG PET/CT) can detect both anatomical and metabolic information, which is applied in oncologic imaging for diagnosis, staging, and prognosis [11–15]. However, due to the rarity of cardiac masses, ^{18}F-FDG PET/CT does not have an established role in their routine evaluation. In the present study, we retrospectively analysed the ^{18}F-FDG PET/CT images of patients with cardiac masses and sought to evaluate whether this imaging modality could provide useful information on diagnosis and prognosis.

Patients and methods

Patients

The study was approved by the Institutional Review Board. We retrospectively reviewed imaging data of all the patients with cardiac masses who underwent ^{18}F-FDG PET/CT in the PET Center of Union Hospital, Tongji Medical College, Huazhong University of Science and Technology, from August 2012 to August 2018. The inclusion criteria were as follows: (1) age ≥ 18 years and (2) complete clinical and imaging data. The exclusion criterion was diabetic patients or patients with fasting blood glucose ≥ 200 mg/dL. All of the cases were divided into malignant and benign groups according to the histological or long-term follow-up results.

^{18}F-FDG PET/CT protocol

^{18}F-FDG was synthesized with ^{18}F produced by a cyclotron (MINItrace®, GE Healthcare, Milwaukee, WI, USA), with radiochemical purity > 95%. All patients fasted for at least 8 h before the administration of ^{18}F-FDG. A total of 3.70–5.55 MBq (0.10–0.15 mCi)/kg ^{18}F-FDG was administered intravenously. PET/CT was performed approximately 60 min after ^{18}F-FDG administration by a PET/CT scanner (Discovery VCT®, GE Healthcare). Both CT and PET were acquired from the top of the head to the upper thighs. CT scanning was performed after a CT scout view with a tube voltage of 120 kV, a tube current of 110 mAs, and scanning thickness of 3.75 mm. PET was acquired with 3 min per bed position.

PET/CT image interpretation

PET/CT images were visually interpreted by two experienced nuclear medicine physicians in consensus, with knowledge of the initial clinical data but blinded to the histology. The physicians reviewed the CT and PET images and recorded their findings, respectively. The CT diagnosis was mainly according to the location and morphological characteristics of the masses (margin, with/without necrosis), in addition to its relationship with surrounding tissues (with/without infiltration/involvement of epicardium, surrounding tissue, and vessel), with/without pericardial/pleural effusion, and whether there were extracardiac lesions. A semi-quantitative method was applied in the PET interpretation, which was based on several metabolic indices of ^{18}F-FDG uptake (maximum standardized uptake value [SUV_{max}], mean standardized uptake value [SUV_{mean}], metabolic tumour volume [MTV], and total lesion glycolysis [TLG]). All PET and CT data were processed using commercial software (PMOD PNEURO version 3.906, PMOD Technologies Ltd., Zurich, Switzerland) in DICOM format. The lesions were identified on PET images and segmented automatically using a 3D-area growing algorithm in the axial, coronal, and sagittal planes [16]. The measurement of the indices was performed within the regions of interest (ROIs), which were determined by the SUV threshold or from CT image. The SUV threshold was calculated by a background method as described previously [17] as follows:

$$\mathrm{SUVthreshold} = \mathit{S}\mathrm{UVbkgd} + 20\%(\mathrm{SUVmaxROI}-\mathrm{SUVbkgd}), \quad (1)$$

where SUV_{maxROI} refers to SUV_{max} of the lesion and SUV_{bkgd} refers to the mean SUV_{max} of the background. Due to the variability of FDG uptake in the myocardium, we chose the erector spinae muscles as the background. The MTV and SUV_{mean} were determined automatically by the software, and the total lesion glycolysis (TLG) was calculated according to the formula:

$$TLG = SUVmean \times MTV \quad (2)$$

Follow-up

Follow-up was performed after PET/CT scan. During the follow-up time, we recorded the therapeutic response of each patient, the time to first progression/recurrence or death, and the performance status of survivors. OS was defined as the time interval from the date of PET/CT imaging to death related to cardiac mass or the date of last follow-up and was chosen as an endpoint to estimate the prognostic value of clinical data and PET/CT parameters.

Statistical analysis

A commercial software package (SPSS 22.0, IBM Inc., Armonk, NY, USA) was employed for data processing. Continuous variables are expressed as mean ± SD. Categorical variables are expressed as number and percentage. For quantitative data, normal distribution and homogeneity of variances were tested first. Student's *t* test was used for quantitative data with normal distribution and equal variances, while Welch's *t* test was applied if variance was unequal. Quantitative data with non-normal distribution or the categorical variables were compared with the Mann-Whitney *U* test between two groups (benign and malignant groups), or with the Kruskal-Wallis *H* test among three groups (primary, secondary, and lymphoma groups). Receiver operating characteristic (ROC) analysis was used to determine the optimal cutoff values of parameters (SUV_{max}, SUV_{mean}, MTV, and TLG), and the value with the highest sum of sensitivity and specificity was regarded as the cutoff value. Sensitivity, specificity, accuracy, positive predictive value (PPV), and negative predictive value (NPV) were calculated for each variable. The influences of gender, age, morphological features, and metabolic indices were examined in univariate analysis and multivariate Cox regression analysis for overall survival (OS). Kaplan-Meier's method was applied to generate survival curves, and the log-rank test was used for comparison.

Results

The final study population comprised 64 patients (34 men, 30 women; mean age ± SD, 51.20 ± 17.50 years), with 65 cardiac masses (one man with two different benign cardiac masses [myxoma, ventricular aneurysm]). These cardiac masses were diagnosed as follows: (1) malignancy = 38 (58.50%; primary tumours [*N* = 17], metastases [*N* = 15], lymphomas [*N* = 6]); (2) benign = 27 (41.50%; neoplasms [*N* = 13], non-neoplastic lesions [*N* = 12], unknown [*N* = 2]). The information of pathology type, location, related history, and presence of extracardiac lesions is summarized in Table 1, and four representative cases are shown in Fig. 1.

PET/CT findings and diagnostic performance

The comparisons of CT features and FDG metabolic indices between benign and malignant groups, as well as among primary and secondary malignancies and lymphoma, are summarized in Table 2. There were statistically significant differences in multiple morphological features and metabolic indices between the benign and the malignant masses. For malignant masses, among patients with primary or secondary malignancies or lymphoma, there were no statistically significant differences in any of the aforementioned morphological features. The SUV_{max} and SUV_{mean} of lymphoma were significantly higher than those of primary and secondary malignancies (Table 2, Fig. 2a).

Table 2 also illustrates the diagnostic performance of distinguishing benign masses from malignancies using the abovementioned CT features and PET metabolic cutoff values. Each CT feature alone showed relatively low diagnostic accuracy, whereas using a criterion containing more than three CT features for the diagnosis improved the diagnostic performance (sensitivity, 78.94%; specificity, 100%; accuracy, 87.69; PPV, 100%; and NPV, 77.14%). The ROC curves (Fig. 2b) show that using SUV_{max} of 6.75, SUV_{mean} of 3.52, MTV of 61.32, and TLG of 126.07 as cutoff values resulted in the highest diagnostic performance with the areas under the ROC curves (AUC) of 0.9142, 0.8655, 0.8713, and 0.8187, respectively. Multiple logistic regression analysis resulted in

$$\text{logit}(p) = 0.4092 \times \text{SUVmax} + 0.0055 \times \text{TLG} - 3.6223 \quad (3)$$

with a little better AUC than that of SUV_{max} alone (0.9279 vs. 0.9142) (sensitivity, 94.74%; specificity, 85.19%; accuracy, 90.77%; PPV, 90.00%; and NPV, 92.00%), but with no statistical difference.

Combining CT morphological features and SUV_{max} as a criterion for distinguishing benign masses from malignancies optimized the diagnostic performance (≥ 3 CT features and $SUV_{max} \geq 6.75$ [sensitivity, 76.32%; specificity, 100.00%; accuracy, 86.15%; PPV, 100.00%; and NPV, 75.00%]; ≥ 3 CT features or $SUV_{max} \geq 6.75$ [sensitivity, 94.74%; specificity, 88.89%; accuracy, 92.31%; PPV, 92.31%; and NPV, 92.31%]). These results were also shown in Table 2.

Follow-up and Survival Analysis.

Except for two patients with cardiac lipoma who did not undergo surgery, the main treatment for benign lesions was surgery. Surgery with/without adjuvant chemotherapy was the mainstay of treatment for patients with primary cardiac

Table 1 Cardiac lesion pathology, location, related history, and presence or absence of extracardiac lesions

Diagnosis	No.	Location (NO.)							Related history	Extracardiac lesions
		RA	LA	RV	LV	Multiple chambers	Chamber(s) + vessel(s)	Others		
Malignant	38	11	3	2	1	8	12	1	5	28
Primary	17	8	3	–	–	3	3	–	3	8
Angiosarcoma	5	5	–	–	–	–	–	–	–	4
Undifferentiated sarcoma	1	–	1	–	–	–	–	–	1	–
Myofibroblastic sarcoma	1	–	1	–	–	–	–	–	1	1
Synovial sarcoma	1	–	–	–	–	1 (RA + RV)	–	–	1	–
Malignant peripheral nerve sheath tumour	1	–	1	–	–	–	–	–	–	–
Unknown	8	3	–	–	–	2[1]*	3[3]*	–	–	3
Secondary	15	3	–	1	1	2	7	1	2	14
Lung	6	1	–	1	–	–	4[4]*	–	2	6
Mediastinum	6	1	–	–	–	1 (LA + LV)	3 (RA + CS)	1[6]*	–	5
Ovarian cancer	1	1	–	–	–	–	–	–	–	1
Choroidal melanoma	1	–	–	–	–	1 (LA + LV)	–	–	–	1
Esophageal carcinoma	1	–	–	–	1	–	–	–	–	1
Lymphoma	6	–	–	1	–	3[2]*	2[5]*	–	–	6
Benign	27	6	5	3	5	–	2	6	3	2
Neoplasms	13	3	3	1	2	–	2	2	3	1
Myxoma	8	3	3	–	1	–	1 (RA + CI)	–	3	–
Lipoma	2	–	–	–	–	–	–	2[7]*	–	–
Intravenous leiomyomatosis	1	–	–	–	–	–	1 (RA + CI)	–	–	1
Cavernous hemangioma	1	–	–	1	–	–	–	–	–	–
Papillary fibroelastoma	1	–	–	–	1	–	–	–	–	–
Non-neoplastic lesions	12	3	2	–	3	–	–	4	–	1
Thrombus	5	3	2	–	–	–	–	–	–	–
Valvular lesion	4	–	–	–	–	–	–		– 4 (AVJ)	–
Ventricular aneurysm	3	–	–	–	3	–	–	–	–	1[#]
Unknown	2	–	–	2	–	–	–	–	–	–
Total	65	17	8	5	6	8	14	7	8	30

RA, right atrium; *RV*, right ventricle; *LA*, left atrium; *LV*, left ventricle; *CS*, cava superior; *CI*, cava inferior; *AA*, ascending aorta; *PA*, pulmonary artery; *BV*, brachiocephalic vein; *AVJ*, atrioventricular junction; *HV*, hepatic vein

[1] * RA+RV; RA+LA; [2] * RA+RV(2); RA+RV+LA(1); [3] * RA+CS+left BV; RA+ CS+CI+PA+AA; RA+ CI; [4] * RA+CS; RA+CS+jugular vein; LA+ RPA; [5] * RA+ RV+CS(1); RA+CI+HV(1); [6] *intrapericardial; [7] *LV inferior wall (1); interventricular septum (1); [#] a man with stage IV lung cancer

malignancy. The patients with secondary malignancy and lymphoma mainly received systemic chemotherapy.

Because 18 patients were lost to follow-up, the survival analysis was performed in 72.31% (47/65) of cardiac masses, with a mean age of 52.89 ± 17.73 years. The follow-up time ranged from 6 to 2289 days (534 ± 563 days). Of the 47 cardiac masses, 25 were malignant and 22 were benign. Of the 25 patients with malignant masses, 18 (72.00%) died of the disease, whereas only 2 (9.09%) patients with benign disease died. The 2-year OS rates of patients in the malignant and benign groups were 21% and 86%, respectively.

The optimal cutoff values were calculated by ROC curves and are summarized in Table 3. On univariate analysis (Table 3), risk of death was increased for patients with surrounding tissue infiltration, epicardial infiltration, necrosis, multiple chambers or vessel involvement, extracardiac lesion, $SUV_{max} \geq 6.715$, $SUV_{mean} \geq 3.16$, MTV ≥ 54.54, and TLG ≥ 137.90. Irregular mass margins seemed to increase the risk of death but not to a statistically significantly extent (hazard ratio 4.15, $p = 0.056$). Gender, age, pericardial effusion, and pleural effusion were not predictive of overall survival. Multivariate Cox regression analysis showed $SUV_{max} \geq 6.715$ was the only significantly independent prognostic factor ($p < 0.001$).

Kaplan-Meier curves illustrated that the cases with $SUV_{max} < 6.715$ had longer OS than the patients with $SUV_{max} \geq 6.715$, with median survival times of 1460 and 342 days, respectively

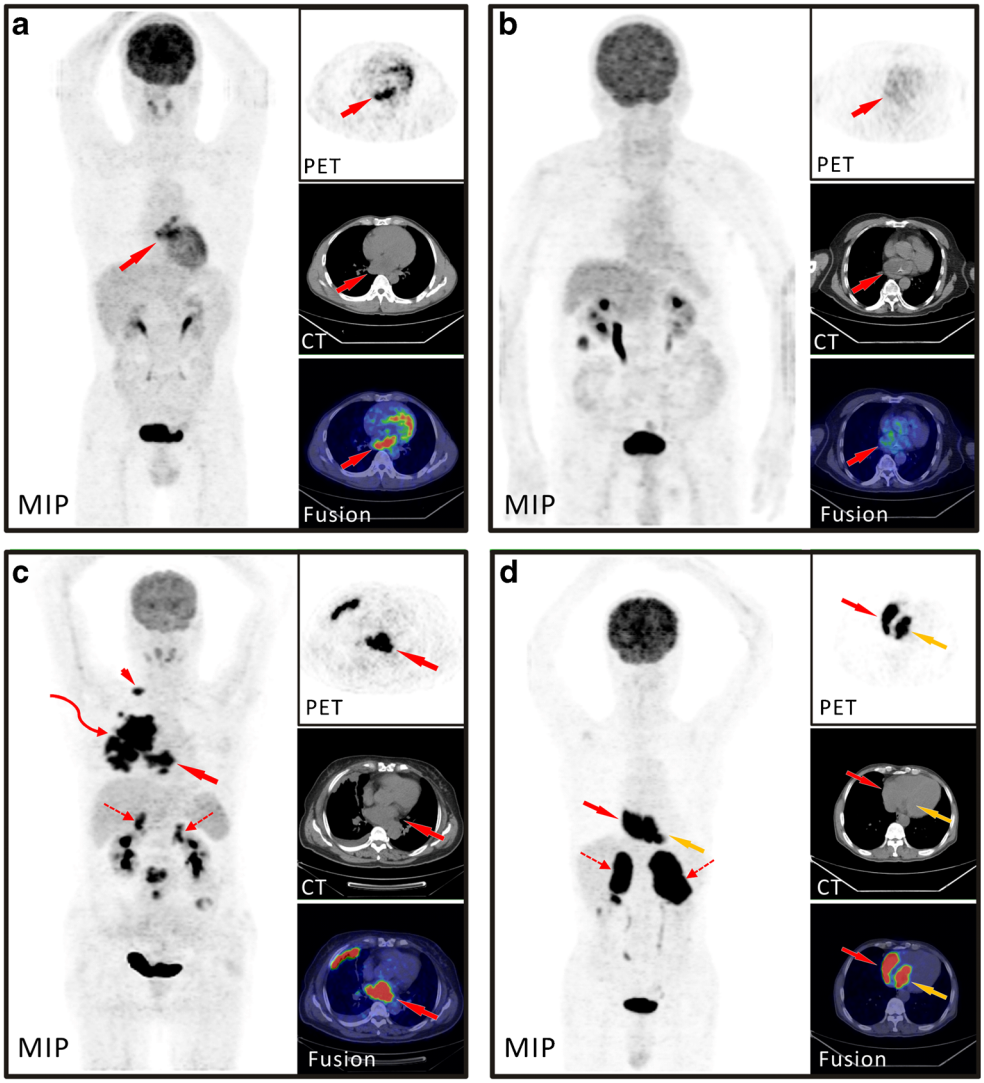

Fig. 1 Representative cases. **a** A 54-year-old man presenting with malignant peripheral nerve sheath tumour in the left atrium. ^{18}F-FDG PET/CT images showed the cardiac tumour with an SUV_{max} of 12.27 without extracardiac involvement (arrows). **b** A 83-year-old man presenting with left atrial myxoma with calcification. Images showed the benign mass with an SUV_{max} of 4.51 (arrows). **c** The ^{18}F-FDG PET/CT images of a 63-year-old woman demonstrated a left atrial hypermetabolic mass with an SUV_{max} of 15.15 (arrows), which was secondary to a malignant mesenchymal tumour in the right lung (curved arrow). The MIP image also detected lymph nodes (arrowhead) and adrenal (dotted arrows) metastases. **d** ^{18}F-FDG PET/CT images of a 61-year-old man revealed a large cardiac mass with an SUV_{max} of 25.37 involving the left atrium (yellow arrows), right atrium (red arrows), and right ventricle (not shown). Bilateral adrenal involvement (dotted arrows) was also noted. The histological diagnosis was diffuse large B cell lymphoma

($p = 0.00016$) (Fig. 3a). Seventeen of the 24 patients with $SUV_{max} \geq 6.715$ (70.83%) died, whereas only three of the 23 lesions in 22 patients with $SUV_{max} < 6.715$ died (13.64%), including one patient with myxoma who died during surgery, one patient with thrombus who died 1 year after heart transplantation due to restrictive cardiomyopathy, and another case with ovarian cancer metastatic to the right atrium. The 2-year OS rates were 29.17% (7/24) in the patients with $SUV_{max} \geq 6.715$ and 86.96% (20/23) in the patients with $SUV_{max} < 6.715$, respectively.

Compared with PET ($SUV_{max} \geq 6.715$)- or CT (≥ 3 features)-positive findings alone, the cases with both PET-positive and CT-positive results had a worse prognosis ($p = 0.0023$) (Fig. 3b). For disease types, statistically significant differences were observed among the subgroups for survival probability, with best survival in the benign group, followed by the lymphoma group. Primary cardiac malignancies had the worst prognosis ($p < 0.001$) (Fig. 3c).

Discussion

^{18}F-FDG PET/CT has been well documented in the diagnosis, staging, and monitoring of neoplastic and some non-neoplastic diseases [18–20]. Given the rarity and complexity of cardiac masses, the values of PET/CT in cardiac masses, especially the prognosis assessment value, remain to be confirmed. Scattered case reports have noted that FDG PET/CT can visualize cardiac masses and assess their glucose metabolism levels [21–28]. A few publications involved cardiac masses cohort showed that PET/CT or PET/MRI with ^{18}F-FDG is promising for differentiating benign from malignant cardiac lesions [29–32]. However, the enrolled patient numbers were limited, ranging from 20 to 24, and prognostic assessment was not available.

In this study, we enrolled 65 cardiac masses in 64 cases for evaluating not only the diagnostic accuracy but also the prognostic value of FDG PET/CT. Considering that non-neoplastic lesions, including thrombus, vegetation, valvular lesions, and

Table 2 Comparison of morphological features and metabolic indices among groups and diagnostic performance

		Benign	Malignant	*p*	Sen. (%)	Spe. (%)	Acc. (%)	PPV (%)	NPV (%)	Primary	Secondary	Lymphoma	*P*
Number		27	38							17	15	6	
Male (%)		16 (59.3%)	19 (50%)	0.461						9 (52.9%)	8 (53.3%)	2 (33.3%)	0.680
Age		51.81 ± 17.47	50.61 ± 17.50	0.784						46.35 ± 18.56	54.13 ± 16.48	53.83 ± 17.05	0.414
CT features	Surrounding tissue infiltration	1	21	0.000	55.26	96.30	72.31	95.45	60.47	8 (47.1%)	8 (53.3%)	5 (83.33%)	0.311
	Involvement of epicardium	0	21	0.000	55.26	100.00	73.85	100.00	61.36	9 (52.9%)	8 (53.3%)	4 (66.67%)	0.833
	Irregular margin	10	38	0.000	100.00	62.96	84.62	79.17	100.00	17 (100%)	15 (100%)	6 (100%)	_
	Presence of necrosis	0	9	0.007	23.68	100.00	55.38	100.00	48.21	5 (29.4%)	2 (13.3%)	2 (33.3%)	0.480
	Pericardial effusion	3	21	0.000	55.26	88.89	69.23	87.50	58.53	6 (35.3%)	10 (66.7%)	5 (83.33%)	0.071
	Pleural effusion	3	18	0.002	47.37	88.89	64.62	85.71	54.55	5 (29.4%)	8 (53.3%)	5 (83.33%)	0.068
	Involvement > 1 chamber or vessel(s)	2	20	0.000	52.63	92.59	69.23	90.91	65.79	6 (35.3%)	9 (60.0%)	5 (83.33%)	0.104
	More than 3 features	0	30	0.000	78.94	100	87.69	100.00	77.14	12 (70.6%)	12 (88.2%)	6 (100%)	0.173
PET features	SUV_{max}	5.25 ± 2.63	11.64 ± 5.14	0.000	92.11	88.89	90.77	92.11	88.89	11.10 ± 4.67	10.01 ± 3.92	17.26 ± 5.98	0.008
	SUV_{mean}	2.94 ± 1.49	5.08 ± 2.11	0.000	78.95	85.19	81.34	88.24	74.19	4.59 ± 1.59	4.51 ± 1.57	7.87 ± 2.58	0.001
	MTV	20.61 ± 23.89	129.47 ± 136.54	0.000	55.26	96.30	72.31	95.45	60.47	114.85 ± 115.25	124.77 ± 160.73	182.63 ± 137.58	0.583
	TLG	58.12 ± 78.30	709.4 ± 851.96	0.000	73.68	92.59	81.54	93.33	71.43	612.64 ± 876.23	578.08 ± 795.27	1311.86 ± 790.11	0.169
CT and PET features	CT ≥ 3 features AND SUV_{max} ≥ 6.75	0	29	0.000	76.32	100.00	86.15	100.00	75.00	12 (70.6%)	11 (73.33%)	6 (100%)	0.165
	CT ≥ 3 features OR SUV_{max} ≥ 6.75	3	36	0.000	94.74	88.89	92.31	92.31	92.31	17 (100%)	13 (86.67%)	6 (100%)	0.143

Sen, sensitivity; *Spe*, specificity; *Acc*, accuracy; *PPV*, positive predictive value; *NPV*, negative predictive value

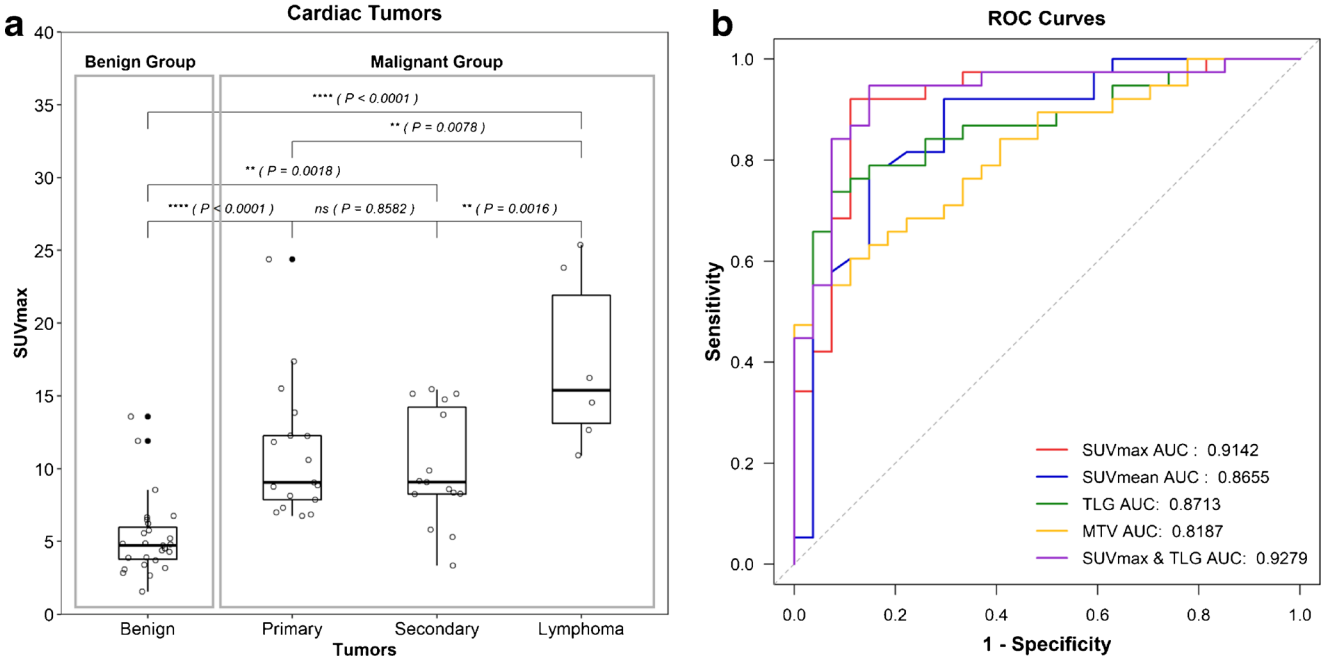

Fig. 2 **a** SUV_{max} of different types of cardiac masses. **b** ROC curve of SUV_{max}, SUV_{mean}, TLG, MTV, and SUV_{max} and TLG

ventricular aneurysm, sometimes mimic tumours [33–35], we brought the patients with the abovementioned tumour mimics into this retrospective study. There are considerable differences in treatment strategies not only between malignant and benign entities but also among different types of malignancies. Therefore, in addition to diagnostic and prognostic assessment between malignant and benign entities, distinguishing among primary malignancies, secondary malignancies, and lymphoma was also carried out in our study.

Our results suggest that ^{18}F-FDG PET/CT is a reliable tool in the diagnosis of cardiac masses. From the results of this study, we propose an ^{18}F-FDG PET/CT diagnostic approach for cardiac masses shown in Fig. 4. Some reports have suggested that a location of the tumour outside the left heart, tissue inhomogeneity, the presence of pericardial effusion, infiltrative growth pattern, and lobulated margins are predictors of malignant cardiac masses [8–10, 36, 37]. Tumour size is not efficient to differentiate benign masses from malignancies [8, 32]. Following the morphological score system established by Rahbar et al. [32], we enrolled multiple morphological features for analysis (Table 2). Our data showed the diagnostic performance of combining ≥3 CT features was relatively superior to those using a single feature.

Table 3 Results of univariate analysis for predicting overall survival

	Optimal cutoff value	AUC	Hazard ratio	95% CI	*p* value
Gender	–	–	1.11	0.46–2.68	0.819
Age	–	–	1.02	0.99–1.05	0.170
Surrounding tissue infiltration	–	–	3.98	1.62–9.81	0.003**
Epicardial infiltration	–	–	2.92	1.20–7.08	0.018*
Irregular margin	–	–	4.15	0.96–17.92	0.056
Necrosis	–	–	2.72	1.08–6.83	0.033*
Pericardial effusion	–	–	2.38	0.98–5.77	0.055
Pleural effusion	–	–	2.10	0.87–5.07	0.098
Multi chambers/vessels	–	–	2.54	1.05–6.15	0.038*
Extracardiac lesion	–	–	2.75	1.12–6.75	0.027*
SUV_{max}	6.715	0.7574	7.61	2.21–26.20	0.001**
SUV_{mean}	3.16	0.7343	6.23	1.81–21.40	0.004**
MTV	54.54	0.7185	2.97	1.210–7.28	0.017*
TLG	137.90	0.7019	3.32	1.32–8.35	0.011*

*, $p < 0.05$; **, $p < 0.01$

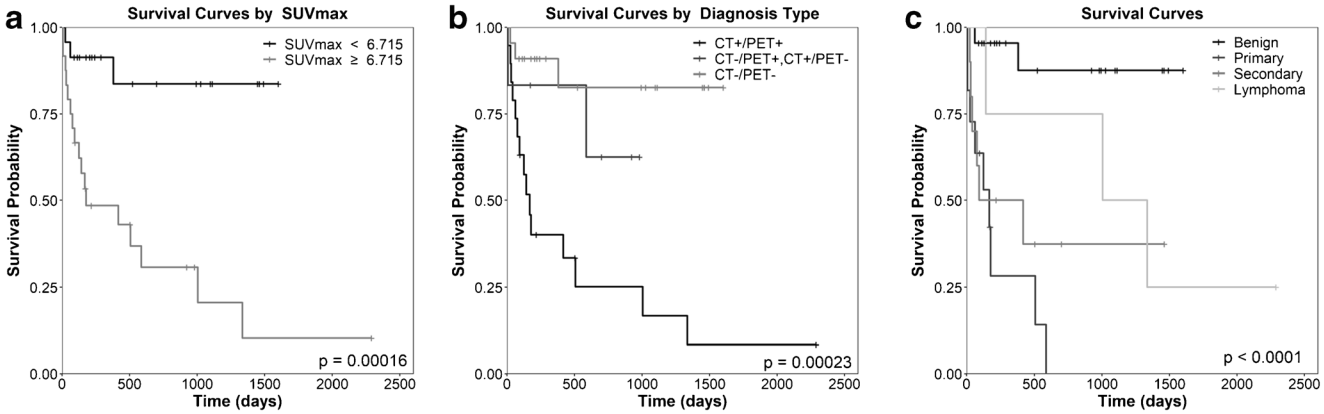

Fig. 3 Kaplan-Meier analysis of the relationship between OS and SUV_{max} (**a**), PET/CT findings (**b**), and mass types (**c**), respectively

The lesion SUV_{max} values in this study were significantly higher in malignant cardiac masses than those in benign lesions, which is similar to those in the studies (imaging modality, patient numbers; SUV_{max} cutoff value; sensitivity, specificity, accuracy, PPV, and NPV for diagnosis) conducted by Shao et al. [29] (PET/CT; $N = 23$; 3.5–4.0; 100.0%, 90%, 95.7%, 92.9%, and 100.0%), Rahbar et al. [32] (PET/CT, $N = 24$; 3.5; 100%, 86%, 96%, 100%, and 100%), and Nensa et al. [30] (PET/MR, $N = 20$; 5.2; 100%, 92%, 95%, 88%, and 100%). The cutoff value in our study (6.75) was higher than those of the abovementioned three publications, whereas the diagnostic performance (92.11%, 88.89%, 90.77%, 92.11%, and 88.89%) using $SUV_{max} \geq 6.75$ seemed to be slightly inferior to those studies. These differences might be due to the larger sample size and intra-individual/individual variability. Notably, we hold an identical view with these reports that despite an SUV_{max} of 2.5 being the conventional cutoff for differentiating benign and malignant lesions in other solid tumours, it is not suitable for cardiac masses. Additionally, SUV_{mean}, MTV, and TLG also reflect glycometabolism and were used for diagnosis [38–40] as we did in our study. However, these values had relatively lower efficiency in diagnostic accuracy compared with SUV_{max}.

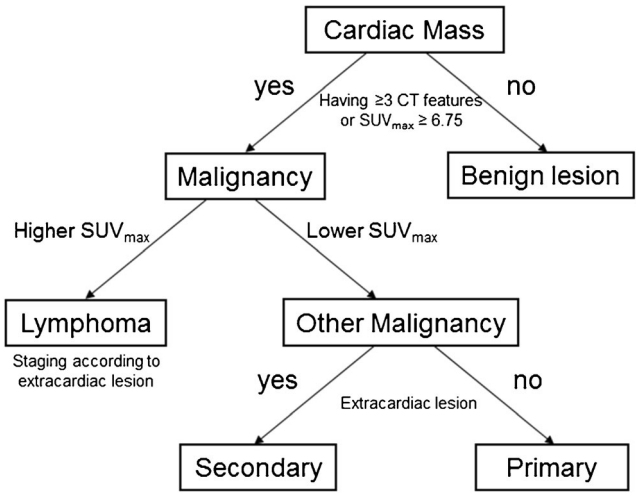

Fig. 4 FDG PET/CT diagnostic approach for cardiac masses. First, using $SUV_{max} \geq 6.75$ or ≥ 3 CT features as a differential criterion to distinguish malignancies from benign masses. Second, lymphoma may be distinguished from other malignancies by a higher FDG uptake. Moreover, further detection of extracardiac lesions can not only stage lymphoma but also identify primary and secondary malignant masses

Simultaneous consideration of CT results (≥ 3 features) and SUV_{max} (≥ 6.75) could further optimize the diagnostic performance (Table 2). If both CT- and SUV_{max}-positive results were regarded as positive criteria, the specificity and PPV would increase, avoiding false-positive results. In contrast, either CT- or SUV_{max}-positive results regarded as positive criteria could increase the sensitivity and NPV, reducing false-negative results.

In addition to providing morphological characteristics and metabolic parameters, ^{18}F-FDG PET/CT clearly illustrated the locations of the lesions, which was critical for diagnosis and staging. Our results suggest cardiac masses may occur in any single chamber or multiple chambers, with or without vascular infiltration. The right atrium is the most common location for both malignant and benign cardiac masses. Multi-chambers or vessel involvement often occurred in malignant disease. In benign diseases, only one case of myxoma and one case of intravenous leiomyomatosis occurred in the right atrium and inferior vena cava. Some diseases had specific locations, such as lipomas usually occurring in the myocardial wall, valvular lesions in the atrioventricular junction area, and ventricular aneurysms in the ventricle (more common in left ventricle) [4]. One of the biggest advantages of PET/CT is panoramic imaging, which is especially useful for detecting tumours in patients with metastasis with unknown primary and for staging. In this study, PET/CT detected extracardiac lesions in 30 cases, contributing to correct staging.

Diagnostic CT and MR (especially cardiac MR) provide excellent anatomical visualization [41, 42], and some criteria (surrounding tissue infiltration, epicardial infiltration, necrosis, multiple chambers or vessel involvement, and extracardiac lesions) were associated with poorer OS. However, multivariate Cox regression analysis showed all of the

abovementioned morphological criteria were not independent prognostic factors. In addition to morphological criteria, PET/CT offers semi-quantitative metabolic indices to aid prognostic assessment. Due to the panoramic view of PET/CT, the detection of extracardiac lesions allows prognostic evaluation. High glycometabolism levels indicate worse outcome, as is reported in other solid tumours [43, 44]. Our data demonstrated that SUV_{max} is the only significant independent prognostic factor. The patients with cardiac masses with $SUV_{max} \geq 6.715$ had a significantly worse prognosis.

In this study, patients with benign masses had the best prognosis, because gross total resection could alleviate the heart burden and greatly improve the quality of life, obtaining satisfactory long-term survival [45, 46]. Primary cardiac lymphoma had a relatively favourable prognosis due to most patients having a good response to chemotherapy. Petrich et al. [47] described poor survival with left ventricular involvement by lymphoma. However, no left ventricular involvement was observed in our study, which may be one of the reasons for the relatively good prognosis. Whether primary or secondary, cardiac malignancies have a very dismal prognosis because of their high degree of aggressiveness [46]. Some authors suggest right heart malignancies tend to be bulky, infiltrative, cause late symptoms, and metastasize early, all of which are closely related to poor outcome [48, 49]. The majority of our cases had right cardiac involvement, which could partly explain the poor prognosis. Superior survival was observed in secondary malignancies in comparison with primary ones, which might be due in part to the pathological type of primary tumour and relatively good response to therapy.

One of the main limitations of this study is the background interference coming from physiological uptake of ^{18}F-FDG in myocardium in some patients. A low-carbohydrate/high-fat diet before ^{18}F-FDG administration can suppress the tracer accumulation within the myocardium [50, 51]. However, this diet regimen was not instituted due to the lack of suspicion of a cardiac mass. Prolonged fasting before ^{18}F-FDG PET is another suitable method to depress normal myocardial ^{18}F-FDG uptake [51, 52], which was performed in our study. Other limitations include inexact image fusion due to the respiratory and cardiac motion [53], the relatively short follow-up time, and the heterogeneity of treatment modalities. In addition, although our study enrolled 64 cases, which is a relatively larger cohort compared with previous studies, the sample size remains relatively small due to the extremely low incidence of cardiac masses. Hence, we need a prospective randomized trial involving a larger number of patients with gated ^{18}F-FDG PET/CT to further confirm our results.

Conclusions

^{18}F-FDG PET/CT is of great value for diagnosis and prognostic assessment in patients with cardiac masses before treatment and has optimal detecting ability for extracardiac lesions due to the whole-body images. As a semi-quantitative metabolic criterion, $SUV_{max} \geq 6.75$ displayed significant positive predictive value for cardiac malignancies, and $SUV_{max} \geq 6.715$ predicted poor overall survival.

Acknowledgements We thank Libby Cone, MD, MA, from Liwen Bianji, Edanz Group China (www.liwenbianji.cn/ac) for editing a draft of this manuscript.

Funding information This work was supported by the National Natural Science Foundation of China (No. 81873906, 81630049, and 81401444), the Key Project of Hubei Province Technical Innovation (2017ACA182), and the Clinical Research Physician Program of Tongji Medical College, Huazhong University of Science and Technology (No. 5001530008).

Compliance with ethical standards

Conflict of interest The authors declare that they have no conflict of interest.

Research involving human participants and/or animals This retrospective study of existing patient data and images was approved by the institutional review board of Union Hospital, Tongji Medical College, Huazhong University of Science and Technology. The requirement for informed consent was waived.

References

1. Patel J, Sheppard MN. Pathological study of primary cardiac and pericardial tumours in a specialist UK Centre: surgical and autopsy series. Cardiovascular Pathology. 2010;19:343–52. https://doi.org/10.1016/j.carpath.2009.07.005.
2. Centofanti P, Di Rosa E, Deorsola L, Dato GM, Patane F, La Torre M, et al. Primary cardiac tumors: early and late results of surgical treatment in 91 patients. Ann Thorac Surg. 1999;68:1236–41. https://doi.org/10.1016/s0003-4975(99)00700-6.
3. Chiles C, Woodard PK, Gutierrez FR, Link KM. Metastatic involvement of the heart and pericardium: CT and MR imaging. Radiographics. 2001;21:439–49. https://doi.org/10.1148/radiographics.21.2.g01mr15439.
4. Butany J, Nair V, Naseemuddin A, Nair GM, Catton C, Yau T. Cardiac tumours: diagnosis and management. The Lancet Oncology. 2005;6:219–28. https://doi.org/10.1016/S1470-2045(05)70093-0.
5. Bruce CJ. Cardiac tumours: diagnosis and management. Heart. 2011;97:151–60. https://doi.org/10.1136/hrt.2009.186320.
6. Abu Saleh WK, Ramlawi B, Shapira OM, Al Jabbari O, Ravi V, Benjamin R, et al. Improved outcomes with the evolution of a neoadjuvant chemotherapy approach to right heart sarcoma. Ann Thorac Surg. 2017;104:90–6. https://doi.org/10.1016/j.athoracsur.2016.10.054.
7. Hudzik B, Miszalski-Jamka K, Glowacki J, Lekston A, Gierlotka M, Zembala M, et al. Malignant tumors of the heart. Cancer Epidemiol. 2015;39:665–72. https://doi.org/10.1016/j.canep.2015.07.007.
8. Hoffmann U, Globits S, Schima W, Loewe C, Puig S, Oberhuber G, et al. Usefulness of magnetic resonance imaging of cardiac and paracardiac masses. Am J Cardiol. 2003;92:890–5. https://doi.org/10.1016/s0002-9149(03)00911-1.

9. Esposito A, De Cobelli F, Ironi G, Marra P, Canu T, Mellone R, et al. CMR in the assessment of cardiac masses: primary malignant tumors. J Am Coll Cardiol Img. 2014;7:1057–61. https://doi.org/10.1016/j.jcmg.2014.08.002.
10. Araoz PA, Mulvagh SL, Tazelaar HD, Julsrud PR, Breen JF. CT and MR imaging of benign primary cardiac neoplasms with echocardiographic correlation. Radiographics. 2000;20:1303–19. https://doi.org/10.1148/radiographics.20.5.g00se121303.
11. Saif MW, Tzannou I, Makrilia N, Syrigos K. Role and cost effectiveness of PET/CT in management of patients with cancer. The Yale journal of biology and medicine. 2010;83:53–65.
12. Bar-Shalom R, Yefremov N, Guralnik L, Gaitini D, Frenkel A, Kuten A, et al. Clinical performance of PET/CT in evaluation of cancer: additional value for diagnostic imaging and patient management. Journal of nuclear medicine. 2003;44:1200–9.
13. Zaucha JM, Chauvie S, Zaucha R, Biggii A, Gallamini A. The role of PET/CT in the modern treatment of Hodgkin lymphoma. Cancer Treat Rev. 2019;77:44–56. https://doi.org/10.1016/j.ctrv.2019.06.002.
14. Lue KH, Wu YF, Liu SH, Hsieh TC, Chuang KS, Lin HH, et al. Prognostic value of pretreatment radiomic features of 18F-FDG PET in patients with Hodgkin lymphoma. Clin Nucl Med. 2019. https://doi.org/10.1097/RLU.0000000000002732.
15. Gouw ZAR, La Fontaine MD, van Kranen S, van de Kamer JB, Vogel WV, van Werkhoven E, et al. The prognostic value of baseline 18F-FDG PET/CT in human papillomavirus-positive versus human papillomavirus-negative patients with oropharyngeal cancer. Clin Nucl Med. 2019;44:e323–e8. https://doi.org/10.1097/RLU.0000000000002531.
16. Choi WH, Um YH, Jung WS, Kim SH. Automated quantification of amyloid positron emission tomography: a comparison of PMOD and MIMneuro. Ann Nucl Med. 2016;30:682–9. https://doi.org/10.1007/s12149-016-1115-6.
17. Liao S, Lan X, Cao G, Yuan H, Zhang Y. Prognostic predictive value of total lesion glycolysis from 18F-FDG PET/CT in postsurgical patients with epithelial ovarian cancer. Clin Nucl Med. 2013;38:715–20. https://doi.org/10.1097/RLU.0b013e31829f57fa.
18. Weber WA. Assessing tumor response to therapy. Journal of nuclear medicine. 2009;50(Suppl 1):1S–10S. https://doi.org/10.2967/jnumed.108.057174.
19. Brown PJ, Zhong J, Frood R, Currie S, Gilbert A, Appelt AL, et al. Prediction of outcome in anal squamous cell carcinoma using radiomic feature analysis of pre-treatment FDG PET-CT. Eur J Nucl Med Mol Imaging. 2019. https://doi.org/10.1007/s00259-019-04495-1.
20. Zhuang H, Codreanu I. Growing applications of FDG PET-CT imaging in non-oncologic conditions. J Biomed Res. 2015;29:189–202. https://doi.org/10.7555/jbr.29.20140081.
21. Hori Y, Funabashi N, Miyauchi H, Nakagawa K, Shimura H, Miyazaki M, et al. Angiosarcoma in the right atria demonstrated by fusion images of multislice computed tomography and positron emission tomography using F-18 fluoro-deoxyglucose. Int J Cardiol. 2007;123:e15–7. https://doi.org/10.1016/j.ijcard.2006.11.093.
22. Moulin-Romsee G, De Wever W, Verbeken E, Mortelmans L. Atrial metastasis of esophageal carcinoma detected by follow-up FDG PET/CT. Clin Nucl Med. 2007;32:393–5. https://doi.org/10.1097/01.rlu.0000259639.83809.73.
23. Orcurto MV, Delaloye AB, Letovanec I, Martins Favre M, Prior JO. Detection of an asymptomatic right-ventricle cardiac metastasis from a small-cell lung cancer by F-18-FDG PET/CT. Journal of thoracic oncology. 2009;4:127–30. https://doi.org/10.1097/JTO.0b013e318189f60e.
24. Vatankulu B, Dirlik Serim B, Sonmezoglu K, Vatankulu MA. Right ventricle metastasis of pleomorfic undifferentiated sarcoma detected by FDG PET/CT and three-dimensional echocardiography. Echocardiography. 2016;33:1103–4. https://doi.org/10.1111/echo.13241.
25. Crombe A, Lintingre PF, Le Loarer F, Lachatre D, Dallaudiere B. Multiple skeletal muscle metastases revealing a cardiac intimal sarcoma. Skelet Radiol. 2018;47:125–30. https://doi.org/10.1007/s00256-017-2768-5.
26. Tan H, Jiang L, Gao Y, Zeng Z, Shi H. 18F-FDG PET/CT imaging in primary cardiac angiosarcoma: diagnosis and follow-up. Clin Nucl Med. 2013;38:1002–5. https://doi.org/10.1097/RLU.0000000000000254.
27. Hod N, Shalev A, Levin D, Anconina R, Ezroh Kazap D, Lantsberg S. FDG PET/CT of cardiac angiosarcoma with pulmonary metastases. Clin Nucl Med. 2018;43:744–6. https://doi.org/10.1097/RLU.0000000000002215.
28. Jiang Y, Ma X, Tan Y, Lu Q, Wang Y. Hamartoma of mature cardiac myocytes mimicking malignancy on 18F-FDG PET/CT images. Clin Nucl Med. 2019. https://doi.org/10.1097/RLU.0000000000002679.
29. Shao D, Wang SX, Liang CH, Gao Q. Differentiation of malignant from benign heart and pericardial lesions using positron emission tomography and computed tomography. Journal of Nuclear Cardiology. 2011;18:668–77. https://doi.org/10.1007/s12350-011-9398-4.
30. Nensa F, Tezgah E, Poeppel TD, Jensen CJ, Schelhorn J, Kohler J, et al. Integrated 18F-FDG PET/MR imaging in the assessment of cardiac masses: a pilot study. Journal of Nuclear Medicine. 2015;56:255–60. https://doi.org/10.2967/jnumed.114.147744.
31. Yaddanapudi K, Brunken R, Tan CD, Rodriguez ER, Bolen MA. PET-MR imaging in evaluation of cardiac and paracardiac masses with histopathologic correlation. J Am Coll Cardiol Img. 2016;9:82–5. https://doi.org/10.1016/j.jcmg.2015.04.028.
32. Rahbar K, Seifarth H, Schafers M, Stegger L, Hoffmeier A, Spieker T, et al. Differentiation of malignant and benign cardiac tumors using 18F-FDG PET/CT. Journal of Nuclear Medicine. 2012;53:856–63. https://doi.org/10.2967/jnumed.111.095364.
33. Wybraniec MT, Wrobel W, Myszor J, Mizia-Stec K. Left ventricular diverticulum mimicking cardiac tumor. Echocardiography. 2017;34:1548–51. https://doi.org/10.1111/echo.13584.
34. Yuan SM, Jing H, Lavee J. Tumors and tumor-like lesions of the heart valves. Rare tumors. 2009;1:e35. https://doi.org/10.4081/rt.2009.e35.
35. Rinuncini M, Zuin M, Scaranello F, Fejzo M, Rampin L, Rubello D, et al. Differentiation of cardiac thrombus from cardiac tumor combining cardiac MRI and 18F-FDG-PET/CT imaging. Int J Cardiol. 2016;212:94–6. https://doi.org/10.1016/j.ijcard.2016.03.059.
36. Krombach GA, Spuentrup E, Buecker A, Mahnken AH, Katoh M, Temur Y, et al. Heart tumors: magnetic resonance imaging and multislice spiral CT. RoFo : Fortschritte auf dem Gebiete der Rontgenstrahlen und der Nuklearmedizin. 2005;177:1205–18. https://doi.org/10.1055/s-2005-858489.
37. Grebenc ML, Rosado de Christenson ML, Burke AP, Green CE, Galvin JR. Primary cardiac and pericardial neoplasms: radiologic-pathologic correlation. Radiographics. 2000;20:1073–103; quiz 110–1, 112. https://doi.org/10.1148/radiographics.20.4.g00jl081073.
38. Laffon E, de Clermont H, Lamare F, Marthan R. Variability of total lesion glycolysis by 18F-FDG-positive tissue thresholding in lung cancer. Journal of Nuclear Medicine Technology. 2013;41:186–91. https://doi.org/10.2967/jnmt.113.122952.
39. Chen HH, Chiu NT, Su WC, Guo HR, Lee BF. Prognostic value of whole-body total lesion glycolysis at pretreatment FDG PET/CT in non-small cell lung cancer. Radiology. 2012;264:559–66. https://doi.org/10.1148/radiol.12111148.
40. Yan H, Zhou X, Wang X, Li R, Shi Y, Xia Q, et al. Delayed (18)F FDG PET/CT imaging in the assessment of residual tumors after

transurethral resection of bladder cancer. Radiology. 2019;190032. https://doi.org/10.1148/radiol.2019190032.

41. Liddy S, McQuade C, Walsh KP, Loo B, Buckley O. The assessment of cardiac masses by cardiac CT and CMR including pre-op 3D reconstruction and planning. Curr Cardiol Rep. 2019;21:103. https://doi.org/10.1007/s11886-019-1196-7.
42. Lichtenberger JP 3rd, Dulberger AR, Gonzales PE, Bueno J, Carter BW. MR imaging of cardiac masses. Topics in Magnetic Resonance Imaging. 2018;27:103–11. https://doi.org/10.1097/RMR.0000000000000166.
43. Cegla P, Burchardt E, Roszak A, Czepczynski R, Kubiak A, Cholewinski W. Influence of biological parameters assessed in [18F] FDG PET/CT on overall survival in cervical cancer patients. Clin Nucl Med. 2019. https://doi.org/10.1097/rlu.0000000000002733.
44. Xu M, Wang L, Ouyang M, Lin J, Wang L, Zheng X, et al. Prediction of lymph node metastasis by PET/CT metabolic parameters in patients with esophageal squamous cell carcinoma. Nucl Med Commun. 2019;40:933–9. https://doi.org/10.1097/mnm.0000000000001050.
45. Pacini D, Careddu L, Pantaleo A, Berretta P, Leone O, Marinelli G, et al. Primary benign cardiac tumours: long-term results. European Journal of Cardio-Thoracic Surgery. 2012;41:812–9. https://doi.org/10.1093/ejcts/ezr067.
46. Mo R, Mi L, Zhou Q, Wang D. Outcomes of surgical treatment in 115 patients with primary cardiac tumours: a 15-year experience at a single institution. Journal of Thoracic Disease. 2017;9:2935–41. https://doi.org/10.21037/jtd.2017.08.04.
47. Petrich A, Cho SI, Billett H. Primary cardiac lymphoma: an analysis of presentation, treatment, and outcome patterns. Cancer. 2011;117:581–9. https://doi.org/10.1002/cncr.25444.
48. Blackmon SH, Patel A, Reardon MJ. Management of primary cardiac sarcomas. Expert Rev Cardiovasc Ther. 2008;6:1217–22. https://doi.org/10.1586/14779072.6.9.1217.
49. Vaporciyan A, Reardon MJ. Right heart sarcomas. Methodist DeBakey Cardiovascular Journal. 2010;6:44–8.
50. Boellaard R, Delgado-Bolton R, Oyen WJ, Giammarile F, Tatsch K, Eschner W, et al. FDG PET/CT: EANM procedure guidelines for tumour imaging: version 2.0. Eur J Nucl Med Mol Imaging. 2015;42:328–54. https://doi.org/10.1007/s00259-014-2961-x.
51. Saponara M, Ambrosini V, Nannini M, Gatto L, Astolfi A, Urbini M, et al. (18)F-FDG-PET/CT imaging in cardiac tumors: illustrative clinical cases and review of the literature. Therapeutic advances in medical oncology. 2018;10:1758835918793569. https://doi.org/10.1177/1758835918793569.
52. Shao D, Tian XW, Gao Q, Liang CH, Wang SX. Preparation methods prior to PET/CT scanning that decrease uptake of 18F-FDG by myocardium, brown adipose tissue, and skeletal muscle. Acta radiologica (Stockholm, Sweden : 1987). 2017;58:10–8. https://doi.org/10.1177/0284185116633917.
53. Petibon Y, Sun T, Han PK, Ma C, El Fakhri G, Ouyang J. MR-based cardiac and respiratory motion correction of PET: application to static and dynamic cardiac ^{18}F-FDG imaging. Phys Med Biol. 2019. https://doi.org/10.1088/1361-6560/ab39c2.